FAST SAIL ASSISTED FEEDER CONTAINER SHIP

A Burden, G E Hearn, T Lloyd, S Mockler, L Mortola, I B Shin and **B Smith**, University of Southampton, UK

SUMMARY
An environmentally sustainable fast sail assisted feeder (FSAF) container ship concept with a maximum operational speed of 25 knots has been developed for the 2020 South East (S.E.) Asian and Caribbean feeder container markets. The use of low-carbon and zero-sulphur fuel (liquefied natural gas) and improvements in operational efficiency (cargo handling and scheduling) mean predicted green house gas emissions could be reduced by up to 42% and 40% in the two selected operational regions. The adoption of a *Multi-wing* sail system reduces power requirement by up to 6% at a lower ship speed of 15 knots. Whilst the thrust benefit is lower than initially expected, the additional effect of motion damping from the sail system could be significant. The predicted daily cost savings against typical existing ships are 27% and 33% in S.E. Asian and the Caribbean regions respectively, making the concept both economically and environmentally viable.

1. INTRODUCTION

By 2050, shipping emissions are predicted to increase by between 150% and 250% [Buhaug *et al.*, 2009], putting pressure on new ship designs to be more environmentally sustainable. Whilst regulations exist for certain emissions (e.g. MARPOL Annex VI for NO_x, SO_x and PM), there is no such legislation for CO_2. However, the introduction of performance measures, such as the IMO Energy Efficiency Design Index (EEDI) [IMO, 2005] provides a means of assessing designs from an environmental stand-point.

Container ships are large contributors to global shipping emissions, principally due to their high speed [Buhaug *et al.*, 2009]. The 'efficiencies of scale' principle means that the average size of mainline container ships is increasing, thus improving their 'transport efficiency index' (TEI[1]). There is an opportunity for significant improvement in smaller feeder container ships which are responsible for the transport of containers from regional 'hub ports' to smaller satellite ports, where maximum size is limited by berthing restrictions. Improvements in cargo handling and employing 'just-in-time' arrival have been suggested [Wärtsilä Ship Power R&D, 2009]. In addition, the use of wind auxiliary propulsion on merchant vessels is increasing in popularity, as a way to reduce emissions and costs [NYK, 2010; SkySails, 2010], with potential application to feeder ships.

2. MARKET ANALYSIS

The predicted growth in the feeder container ship market by 2020 was estimated using historic port throughput data from 60 ports, selected from four world regions (the Caribbean, Mediterranean & Middle East, Far East and S.E. Asia) for a period between 1995 and 2008 [Degerlund, 2004; 2006; 2008]. The percentage increase on 2009 levels is indicated in Table 2.1.

Table 2.1 – Predicted feeder container ship market growth by 2020

Region	*Predicted increase (%)*
Caribbean	83.12
Med. / Middle East	100.37
Far East	159.33
South East Asia	67.39
Average	**102.55**

In addition to container throughput data, statistical data detailing routes, basis ship particulars, operational principles, and sea and wind conditions was collected to form the basis of an economic and environmental analysis.

Some key assumptions were made in order to optimise the transport chain efficiency, namely that:

- All containers are transhipped through a hub port with direct return feeder services;
- The same level of consumer service is maintained on 2009 levels regarding sailing frequency;
- The number of ships required on a regional basis is halved in order to reduce port congestion;
- Port congestion will be eliminated and the vessel will conduct its own loading and unloading to minimise delays ;
- There is an initial regional target market share of 10%.

[1] TEI = cargo capacity × speed / installed power

An algorithm described in Burden *et al.* (2010) was followed to determine suitable ship size, and speed on a route by route basis. Statistics were compiled to determine ship particulars that satisfied the requirements of the greatest proportion of routes, suggesting a service speed of 25 knots, cargo capacity of 1250-1300 TEU and a 3000 nm range. It was found that the concept would be most suited to the S.E. Asian and Caribbean regions, where greater efficiency savings can be made due to the longer routes, smaller vessel size required and the inadequacy of the ships currently serving these routes. Thus these regions became the focus of the investigation.

3. INITIAL DEVELOPMENT

3.1 PROPULSION MACHINERY CHOICE

The selection of an appropriate propulsion system and fuel has a direct effect on mass distribution and hull form design, and thus must be considered early on in the design. The main criteria were: high efficiency over a range of operating speeds; low fuel consumption and carbon emissions; and a high degree of manoeuvrability.

This rules out the use of a conventional direct drive low-speed diesel engine, even when used with a controllable-pitch propeller. Medium speed engines used in conjunction with azimuthing drives through an electric propulsion system were deemed more appropriate. This gives the desired manoeuvrability without the need for a rudder and removes the requirement for complex shafting between engine and propeller. Additional advantages of electric propulsion include: flexibility of engine location (see Appendix), thus improving cargo capacity; reduced engine mass; and the ability to run the engines at an optimum speed for a high proportion of time. The main disadvantage of this system is that the gains in efficiency are potentially offset by losses in the electrical distribution system and the high drag of the podded drives.

A significant reduction in carbon emissions is possible with the use of liquefied natural gas (LNG) fuel. The development of 'dual-fuel' diesel-LNG medium speed engines [Wärtsilä Ship Power Technology, 2009] means that this fuel type can be used as part of an electric propulsion system, with a 25-30% reduction in CO_2 emissions [Levander, 2008] and lower specific fuel consumption (SFC). It should be noted however that the volume of LNG required, including containment system, is higher than that of diesel fuel.

Further improvements in propulsive efficiency can be made using a contra-rotating pod (CRP) arrangement (Figure 3.1). This propulsion solution is used on high-speed RoPax vessels, resulting in fuel savings up to 16% [Levander, 2002]. Thus two propulsion options were proposed, allowing hull form design to progress: a CRP arrangement (*Hull A*) and a twin-podded drive arrangement (*Hull B*).

Figure 3.1 – Typical contra-rotating pod[2]

3.2 MASS AND POWERING

Initial estimates of ship mass were made using three different methods, namely:

- An empirical method using Lloyd's equipment numeral with constants prescribed for container ships [Watson and Gilfillan, 1977];
- An empirical method to estimate the lightship mass of container ships [Schneekluth and Bertram, 1987];
- Scaling of basis ships with corrections for a change in dimensions and a change in scantlings [Watson, 1998].

A summary of the mass estimates produced by the three different methods is given in Table 3.1. The maximum variation in the results is 14%.

Table 3.1 – Summary of mass estimates

Method	*Total (tonnes)*
Watson and Gilfillan (1977)	20208
Schneeluth and Bertram (1985)	21629
Scaling basis ships	18961

[2] http://img.nauticexpo.it/images_ne/photo-g/sistema-di-propulsione-elettrica-per-navi-pod-193189.jpg, accessed 16th April 2010.

The use of LNG fuel has a direct influence on the ship mass and mass distribution. A comparison of the fuel mass and volume requirements of LNG and MDO is given in Table 3.2.

Table 3.2 – Capacity and emissions per trip

Fuel	*LNG*	*MDO*	*% diff.*
Mass	157.4 t	209.6 t	-24.9
Volume	384.0 m^3	232.9 m^3	64.9
Cost[3]	USD 73212	USD 134783	-45.7

An initial powering estimate of 25 MW was made using a regression analysis of 170 basis vessels. A summary of the initial particulars is given in Table 3.3.

Table 3.3 – Summary of principal particulars

Particular	*Initial*	*Hull A*	*Hull B*
L_{OA} (m)	170.70	170.70	170.70
L_{WL} (m)	155.40	160.09	160.09
B (m)	26.19	26.20	26.20
D (m)	18.97	18.97	18.97
T (m)	9.00	8.94	8.72
C_B	0.57	0.547	0.55
Δ (tonnes)	21402.00	20466.00	20344.00

3.3 HULL FORM

Two hull forms were designed to investigate the viability of the propulsion options, *Hull A* (Figure 3.2) and *Hull B* (Figure 3.3). The resistance of both hulls has been predicted using Holtrop & Mennen (1982) with an emphasis placed on minimising wave pattern resistance, since this component constitutes approximately 40% of the total resistance at 25 knots. *Hull B* was optimised to minimise wave pattern resistance using *Michlet,* a freeware genetic algorithm.

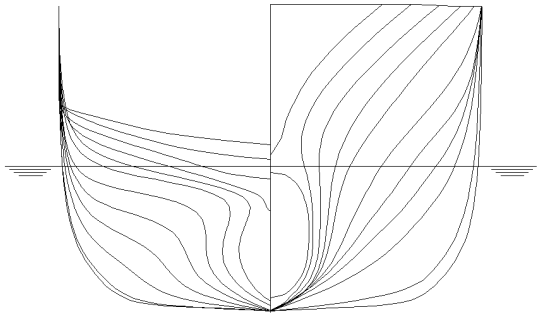

Figure 3.2 – *Hull A* body plan

[3] LNG price taken from Levander (2008); MDO price taken from http://www.bunkerworld.com/prices/ on 23rd March 2010.

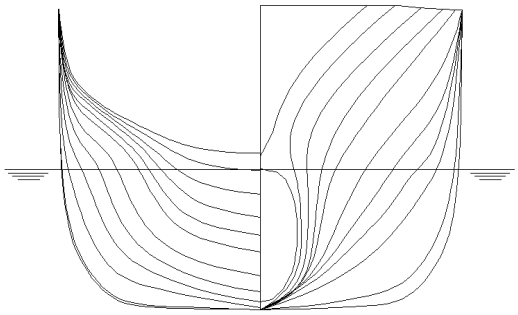

Figure 3.3 – *Hull B* body plan

4. TOWING TANK TESTING RESULTS

Towing tank testing of both hulls provided measurements of upright resistance and added resistance in waves. To investigate the induced resistance and side force resulting from operating in a sailing condition the models were tested at a combination of heel and leeway angles.

4.1 CALM WATER PERFORMANCE

Figure 4.1 shows the upright effective power prediction and measurement for *Hull A* and *Hull B*. It can be seen that *Hull B* performs better in terms of naked hull resistance over the whole range of speeds, largely due to its smaller wetted surface area. Appendages are accounted for in Section 6.2. *Hull B* is poorly represented by the Holtrop regression. This is expected since *Hull B* represents an unconventional merchant ship form.

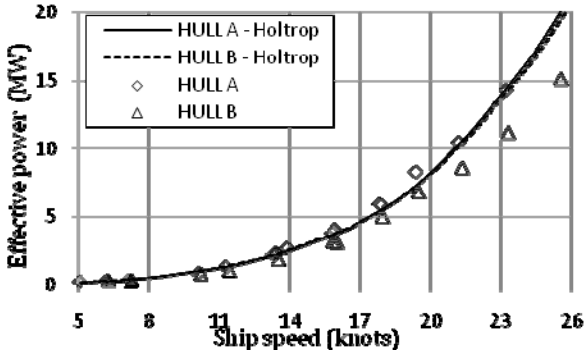

Figure 4.1 – Comparison of experimental and numerical effective power for *Hull A* and *Hull B*

4.3 PERFORMANCE IN WAVES

An assessment of added resistance is particularly important due to the emphasis on tight vessel scheduling. The numerical method proposed by Salvesen (1978) has been used to predict added resistance, using the commercial software *Seakeeper*. Many researchers have noted the

difficulties in modelling the second order nature of added resistance numerically. Consequently it has been measured in regular waves in a towing tank. Figures 4.2 and 4.3 show the non-dimensional added resistance predictions and measurements for *Hull A* and *Hull B* respectively at the two design speeds.

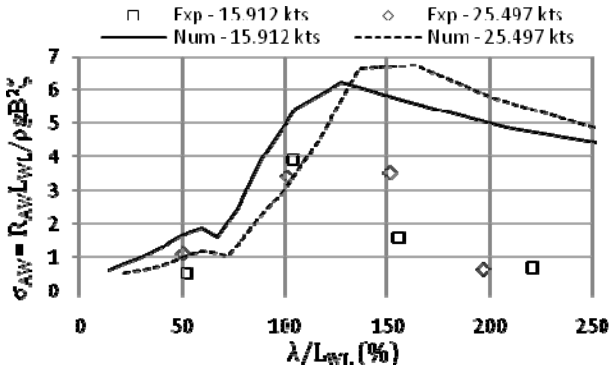

Figure 4.2 – Comparison of numerical and experimental added resistance – *Hull A*

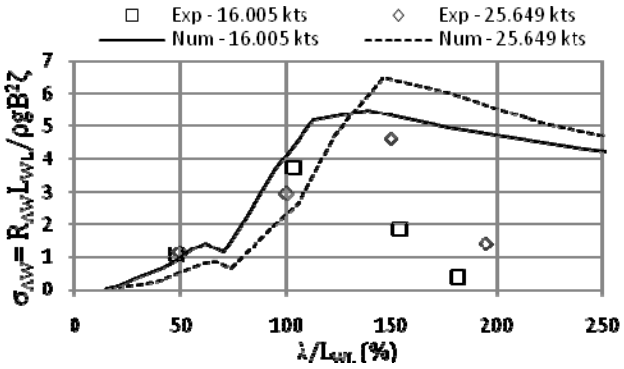

Figure 4.3 – Comparison of numerical and experimental added resistance – *Hull B*

The measured added resistance is important for use in a Performance Prediction Program (PPP) which ultimately allows for the final hull form selection (see Section 6.2).

5. SAIL SYSTEM DESIGN

5.1 INITIAL DESIGN

The sail system is a source of thrust reduction. The drivers in designing a suitable system were readily retractable sails; and improved upwind performance due to a high service speed. A review of conventional (see Table 3 in Schenzle (1985)) and innovative systems from various sources was undertaken. A *Walker Multi-wing* system [Walker, 1985] was chosen due to its superior lift-to-drag ratio. The system consists of three high aspect ratio rigid wings which retract in stormy weather and during cargo handling. One system is located at amidships and another aft (see Appendix).

A NACA0015 wing section with flap at 80% of the chord length was found to give the best lift-to-drag ratio for upwind sailing performance based on an *X-Foil* analysis. The dimensions and aspect ratio were determined considering the dimensional constraints for stowage below the top container stack. The taper ratio was set to one for ease of manufacture of the wind tunnel model. Figure 5.1 illustrates the *Multi-wing* system design with dimensions given in Table 5.1.

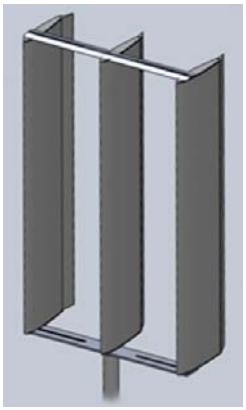

Figure 5.1 – *Multi-wing* system

Table 5.1 – Summary of sail system

No. of systems	2
Height (m)	26.50
Wing span (m)	25.00
Chord (m)	6.25
Aspect Ratio	4.00
Taper Ratio	1.00
Total sail area (m^2)	937.50
Width (m)	13.86
Wing mass (tonnes)	10.00
Linkage structure mass (tonnes)	2.00

Based on the Holtrop regression resistance estimate from Figure 4.1 and aerodynamic coefficients from *X-foil*, 10% and 3% thrust reduction was predicted at ship speeds of 15 and 25 knots respectively.

5.2 WIND TUNNEL MODEL TESTS

Wind tunnel testing was carried out using a 1:15 scale model to determine comprehensive performance estimates investigating the effect of wing spacing, wing stagger and interactions with containers.

5.2.1 Spacing Effect

The spacing between wings was adjustable with 50%, 75%, 100% and 120% of the chord length tested. These configurations were tested up to stalling angle. Figure 5.2 illustrates the 120% spacing configuration which produced maximum lift and drag. As the spacing decreases the lift and drag also decreases, a similar trend to that found in *Biplane Theory* [Munk, 1923]. However, in terms of lift-to-drag ratio, the 100% spacing showed better performance due to low induced drag.

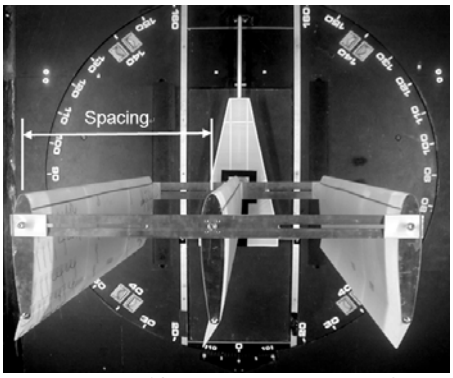

Figure 5.2 – 120% chord spacing configuration

5.2.2 Stagger Effect

The angle of the wings was adjusted to have 0^o, 30^o and 60^o of stagger. Figure 5.3 shows the 30^o stagger case. The tests revealed that 60^o stagger performs best, producing maximum lift, drag and lift-to-drag ratio. Between 30^o and 60^o of stagger the increase in lift is greater than the decrease in lift due to the change in spacing.

5.2.3 Container-sail Interaction Effect

To investigate the aerodynamic interaction between the rig and local container stacks, cardboard boxes were used to simulate containers. It was found that the interaction decreased the induced drag. The top of the containers acted as a reflection plane, decreasing the end vortices on the wings and hence increasing the overall efficiency of the rig.

Figure 5.4 illustrates the increase in the maximum propulsive coefficient, *Cx*. 60^o of stagger was found to increase the efficiency by 20%, whilst the container - sail interactions gave a further 15% improvement.

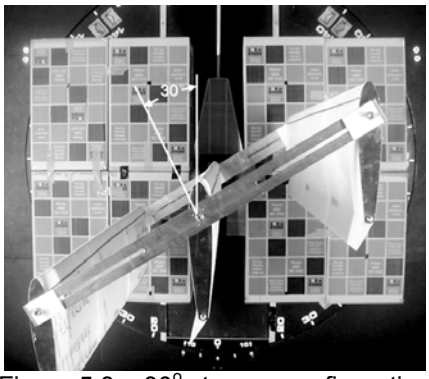

Figure 5.3 – 30^o stagger configuration

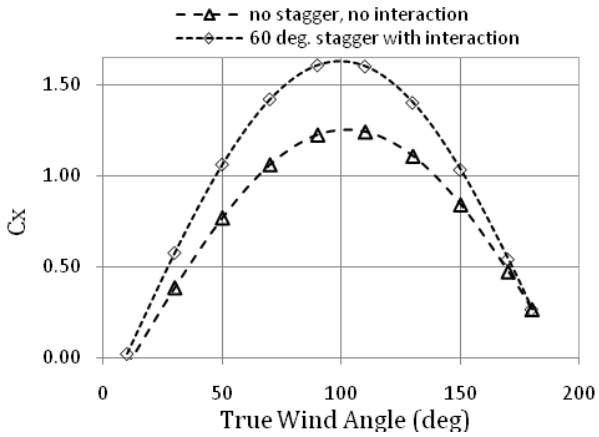

Figure 5.4 – Summary of propulsive benefits of stagger and container sail interactions

5.3 CFD STUDY

Wind tunnel dimensions prevented rig interactions being measured at the selected model scale. Thus the flow interaction between the two rigs was examined using Computational Fluid Dynamics (CFD). A two dimensional full scale model was created to simulate an apparent wind angle of 30^o and a 30 knot wind speed.

The simulation showed that the aft rig experiences a 1.5% decrease in wind speed and 6% lower angle of attack due to the shedding effect of the forward rig. This necessitates optimisation of the aft rig such as increasing the angle of attack to maximise the lift generated.

6. PERFORMANCE PREDICTIONS

6.1 THRUST BENEFIT FROM SAILS

The PPP (see Figure 6.1) was created to combine the various cited experimental results, and estimates the FSAF performance in terms of sail

induced orientations (heel, leeway) and thrust reduction.

The program is used to identify the best wing configuration on an operational basis. The results from the code are then used to simulate 24 selected routes. The wind and sea environments are modelled to include probabilities of wind speed and direction [National Climatic Data Centre, 2009] as well as probability of significant wave height [Hogben, 1986].

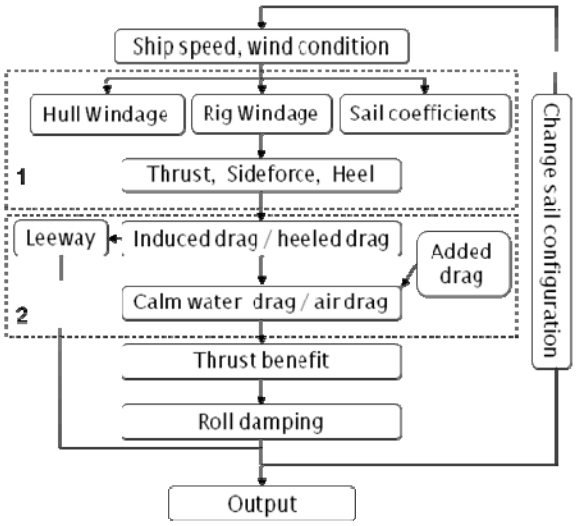

Figure 6.1 – PPP flowchart; aerodynamic index (1) and hydrodynamic index (2)

The main findings are summarised as:

- *Hull A*: 4.1% and 1.5% thrust reduction at 15 and 25 knots respectively;
- *Hull B*: 5.9% and 1.9% thrust reduction at 15 and 25 knots respectively;
- Maximum heel angle: 2.3°;
- Maximum leeway angle: 2.2° for *Hull B.*

The thrust reduction (benefit), *TR*, is calculated according to

$$TR = \frac{Thrust_{nosails} - Thrust_{withsails}}{Thrust_{nosails}} \qquad (6.1)$$

6.2 PROPULSIVE EFFICIENCY

Prediction of the total installed power requirement (P_B) of the two designs requires calculation of the quasi-propulsive coefficient (QPC) and transmission efficiency η_T. The components of the QPC were calculated using empirical formulae (see Burden *et al.* (2010) for a full list of sources used) while η_T was taken as 0.926 by combining the electrical efficiencies of the various components of the electrical distribution system [ABB, 2009].

An empirical method [ITTC, 2008] was used to account for the drag of the podded drives by correcting the open water propeller thrust. To account for the accelerated inflow into the aft propeller of *Hull A*, the advance speed was modified according to Molland *et al.* (2010). Table 6.1 summarises the results, assuming a 15% service margin [ITTC, 2005], for a speed of 25 knots.

Table 6.1 – Summary of propulsive efficiencies.

	Hull A		*Hull B*
	fwd prop	*aft prop*	
QPC	0.85	0.99	0.66
P_B (MW per prop)	12.28	9.82	11.79
P_B (MW inc. margin)	25.42		27.12

Based Table 6.1, *Hull A* has been chosen as the most appropriate given that minimising fuel consumption is a priority. *Hull A* has a 6% lower installed power requirement than *Hull B* at 25 knots. It is also noted that *Hull A* displays lower added resistance (Figures 4.2 and 4.3). The superior thrust benefits of *Hull B* due to the sail system (presented in Section 6.1) are not large enough to offset the propulsion difference in Table 6.1. Thus the following plant were specified: Wärtsilä 50DF medium speed dual-fuel engines, two of 5700 kW and two of 7600 kW [Wärtsilä Ship Power Technology, 2009].

7. FEASIBILITY ASSESSMENT

7.1 OPERATION IN PORT

A key area for improvements in efficiency for the fast feeder concept is port operation. The main concerns are time spent: waiting; manoeuvring; and handling cargo. An estimate of the bow thruster size required to allow berthing without tugs was made, resulting in a 2.65 MW unit being specified. Although large, this reduces the time the vessel takes to berth and saves on tug costs. In addition, the use of gantry cranes is specified, allowing cargo handling fully independent of port facilities. This leads to an estimated 58% reduction in time spent handling cargo, a significant difference for short range feeder services.

7.2 VOYAGE SIMULATION

To compare the efficiency gains of the FSAF concept to typical existing feeder ships, a basic

voyage simulation was carried out, assuming the FSAF would meet the container throughput of two typical vessels. Discussion of the operational profile [Mash, 2009] of the typical vessels was used, as well as basis ship data, to model the typical vessels, with estimates from Sections 6 and 7.1 used to model the FSAF (see Table 6.2). The FSAF is assumed to spend 61% of time underway at 15 knots, and the remainder at 25 knots.

Table 6.2 – Vessel summary for voyage simulation

	S.E. Asia	*Caribbean*	*FSAF*
P_B (MW, 90% MCR)	8280	9660	26600
TEU (90% utilisation)	801	860	1143
Speed (knots, 90% MCR)	15.2	17.0	25.0
Round trip time (hours)	168	168	112
Total TEU (per trip)	3204	3440	3429

The resulting environmental and economic benefits of the FSAF were calculated, as summarised in Table 6.3. Daily cost data was supplied by Ocean Shipping Consultants (2010).

Table 6.3 – Environmental and economic benefits of the FSAF (percentage reduction)

	S.E. Asia	*Caribbean*
CO_2	39.7	42.2
NO_x	89.2	89.7
Fuel cost	51.5	53.4
Total daily cost	29.6	33.3
TEI	63.0	58.0
EEDI	56.0	62.0

It can be seen that the improvements are significant in both regions, making the FSAF both environmentally sustainable and economically viable. Both the TEI and EEDI have been modified to account for the two operating speeds and associated power requirements of the FSAF.

8. SEAKEEPING

8.1 OPERABILITY

The unconventional layout proposed poses concerns over the necessity to voluntarily reduce speed to maintain the crew's ability to function and to prevent excessive loads within container stacks. In order to assess the impact of design choices on the ship operation a number of performance measures were used, namely,

- Motion Sickness Index;
- Subjective Magnitude;
- Motion Induced Interruption;
- Probability of slamming and deck wetness;
- Cargo securing analysis.

The first four performance measures indicated the vessel could operate in sea states up to 5.5m significant wave height (Force 6-7 on Beaufort scale) without requiring a voluntary loss of speed. This exceeds that of typical feeder ships which generally operate unrestricted in sea states up to Force 5 [Mash, 2009].

A cargo securing analysis was conducted using the Regulations for Cargo Securing Arrangements [Lloyd's Register, 2009]. This revealed that container stacks with eight or more containers fail in compression in an oblique sea condition at a container mass below the required nominal mass of 9.3 tonnes. The implications on the design are: a requirement for hatch covers; careful loading procedure; or a reduction in capacity. These measures hamper the fast turnaround of the ship and in the case of the first, add additional mass. The beneficial effect of motion damping from the sails has not been included but could improve the results of this analysis.

8.3 MOTION DAMPING DUE TO SAILS

The aerodynamic roll damping coefficient is calculated using the results of a regression analysis on marine aerofoils based on lifting line theory [Glauhert, 1930]. The reduction in roll of Figure 8.1 is calculated based on Satchwell (1986).

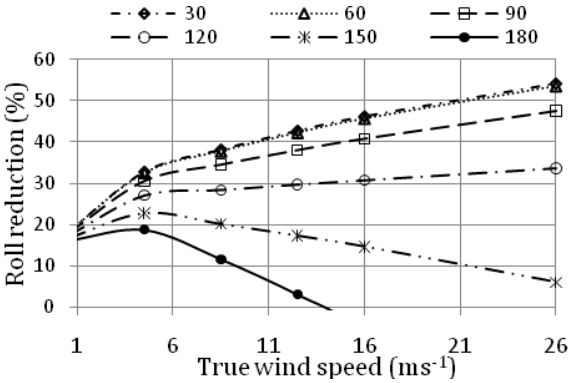

Figure 8.1 – Roll reduction at 25 knots ship speed for a range of apparent wind angles

The PPP shows that on the selected routes an average of 16% and 30% reduction can be achieved at ship speeds of 15 and 25 knots respectively. A reduction in yaw motion is also associated with the

reduction in roll, showing that a decrease in induced resistance can be achieved when sailing to windward. This would provide further economic and environmental benefits, but was not investigated further in this study.

9. STRUCTURAL DESIGN

9.1 GLOBAL STRENGTH

Midship scantlings were derived to meet the requirements of Lloyd's Register and the resulting midship section used to estimate lightship mass. Operational loading conditions were then postulated and the resulting vertical bending moments (VBM) calculated for still water and for the ship balanced on a trochoidal wave crest at its extremities and at midships. The non-dimensionalised VBMs are presented in Figure 9.1, with a comparison to the more conventional container ship *S175* (dashed lines).

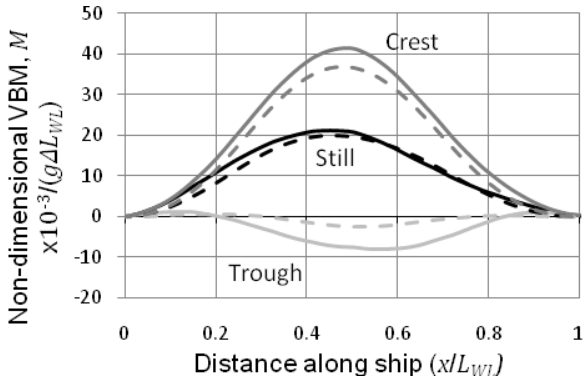

Figure 9.1 – Longitudinal variation in bending moment for FSAF compared to *S175*

Figure 9.1 clearly shows that the effect of moving the accommodation and dividing the machinery mass has been to increase the maximum bending moments experienced, particularly under the influence of waves.

9.2 FE MODELLING

A mandatory requirement for classification of a ship with a novel structure is its strength verification using finite element (FE) methods. The FE analysis program *ANSYS* was used assess a portion of the ships midship section including one sail mast and supporting bulkhead (see Figure 9.2). The ShipRight Procedure for Containerships [LR, 2006] was used to derive suitable loading conditions and to guide the creation of suitable geometry and mesh. The Code for Lifting Appliances [LR, 2008] was used to derive loadings on the sail mast and sails due to ship motion and wind loading.

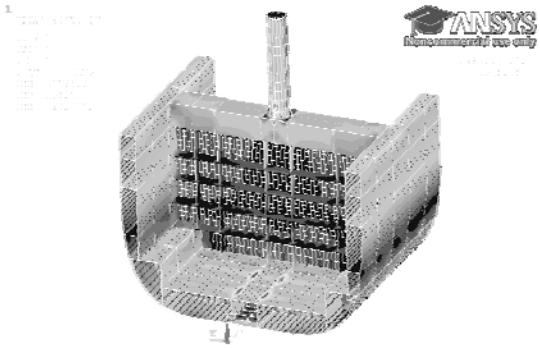

Figure 9.2 – FE model of vessel midship region including bulkhead and sail supporting mast

The FE model allowed the effect of the sails on the strength of the hull to be assessed. In addition, re-design of the mast foundation was possible and mast deflection checked so as not to interfere with neighbouring containers. The results revealed, after a number of design iterations, that the sail had no significant impact on the strength of the hull and that only small areas around the base of the mast (Figure 9.3) failed the criteria of the LR SDA Procedures. The areas of structure that fail could be reduced with more attention paid to the design of the mast intersection with the cross deck.

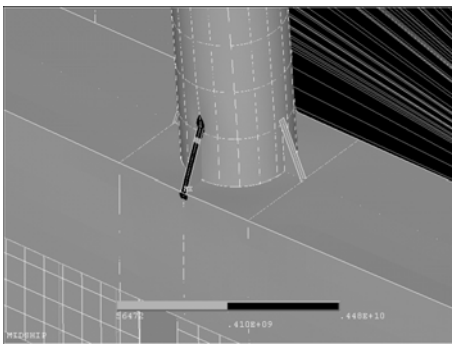

Figure 9.3 – Mast intersection with cross deck and failure region (shaded)

Further FE models were created, representing upwind and downwind sailing conditions, to evaluate the structural performance of a *Multi-wing* system. The pressure applied is derived from a predicted operational wind speed and a worst weather case wind speed of 70 knots, with *X-foil* sail coefficients used.

The analysis revealed that in the operational condition, maximum deflection and stress were acceptable. However, the bottom of the middle stock is highly stress concentrated in the worst weather case for both upwind and downwind conditions. The yield stress limit is exceeded when using an aluminium construction. The rigidity of the bottom bar is also critical in maximum deflection.

10. STABILITY

For the intact stability check, the IMO (2008) code was used, specifically Chapters 3.2 and 4.9. This was applied using the built-in criteria analysis tool in *Hydromax*. Prior to the analysis, the compartments and tanks were defined ensuring trim and draught requirements were satisfied. The FSAF satisfies all criteria with sufficient margins.

Since IMO has no criteria for sail assisted vessels, the LY2 code for monohull sailing yachts [MCA, 2007] was applied to assess the influence of the sails on stability. The concept failed to meet these yacht-based criteria. It was noted that LY2 derives the wind heeling lever differently to the IMO code, using downflooding angle. This implies that an updated code for sail assisted merchant vessels is required to incorporate the effect of sail systems into stability assessment.

11. CONCLUSIONS

Significant improvements in the efficiency of feeder services are possible by taking a more radical approach to ship design and operation. Measures such as changing from MDO to LNG fuel, and eliminating port waiting times have been demonstrated to reduce costs by up to 33% and CO_2 emissions by up to 42%.

Although the use of rigid *Multi-wing* sails contributes low thrust benefit in the case of high speed vessels, their ability to provide motion damping needs further investigation. These effects could both improve seakeeping performance and reduce resistance, thus reducing emissions further.

REFERENCES

ABB (2009) Project Guide for Azipod® VO and VI Series.

Buhaug, Ø., Corbett, J.J., Endresen, Ø., Eyring, V., Faber, J., Hanayama, S., Lee, D.S., Lee, D., Lindstad, H., Markowska, A.Z., Mielde, A., Nelissen, D., Nilsen, J., Palsson, C., Winebrake, J.J., Wu, W. and Yoshida, K. (2009) IMO Second GHG Study 2009, International Maritime Organisation.

Burden, A., Lloyd, T., Mockler, S., Mortola, L., Shin, I.B. and Smith, B. (2010) Concept Design of a Fast Sail Assisted Feeder Container Ship. *Master Thesis.* University of Southampton. Southampton, UK.

Degerlund, J. (2004) *Containerisation Yearbook.* Informa, London, 2004

Degerlund, J. (2006) *ibid 2006*

Degerlund, J. (2008) *ibid 2008*

Glauhert, H. (1930) *The Elements of Airfoil and Airscrew Theory.* Cambridge University Press. Cambridge.

Hogben, N. (1986) *Global Wave Statistics.* Unwin Brothers, Feltham, Middlesex.

Holtrop, J. and Mennen, G.G.J. (1982) An Approximate Power Prediction Method. *ISP*, 29 (335), pp166-70.

International Maritime Organisation (2005) MEPC/Circular.471 - Interim Guidelines for Voluntary Ship CO_2 Emission Indexing for Use in Trials - (29 July 2005) .

International Maritime Organisation (2008) International Code on Intact Stability, Resolution MSC.267(85).

ITTC (2005) Recomended Procedures and Guidelines: 7.5-02-03-01.5 Testing and Extrapolation, Propulsion, Performance, Prediction. Power Margins

ITTC (2008) The Specialist Committee on Azimuthing Podded Propulsion. Proceedings of the 25th ITTC.

Levander, O. (2002) LNG-fuelled RoPax Vessels. *The Ship Power Supplier: Wärtsilä Corporation*, pp10-15.

Levander, O. (2008) Alternative Fuel and Machinery Technologies for Ferries. Proceedings of the RoRo 2008, Gothenburg.

Lloyd's Register (2006) New ShipRight Procedure for Container Ships Helps to Assess Hull Stresses (LR SDA). *Containership Focus*

Lloyd's Register (2008) Code for Lifting Appliances in the Marine Environment.

Lloyd's Register (2009) Lloyd's Register Rules and Regulations - Rules and Regulations for the Classification of Ships.

Mash, C. (2009).Private communication, Nov. 2009.

MCA (2007) LY2 - The Large Commercial Yacht Code. *Maritime and Coastguard Agency.*

Molland, A.F., Turnock, S.R. and Hudson, D.A. (2010) *Ship Resistance and Propulsion.* Cambridge University Press, Cambridge.

Munk, M.M. (1923) *General Biplane Theory*. NACA.

National Climatic Data Centre (2009) NOAA Satellite and Information Service, U.S.

Department of Commerce, Available from: http://www.aoml.noaa.gov/phod/goos.php,
NYK (2010) NYK Super Eco Ship 2030. *http://www.nyk.com/english/csr/envi/ecoship.htm.*
Ocean Shipping Consultants Ltd (2010) Deep-Sea Containership Trading Costs. Obtained from David Tozer of Lloyd's Register with the permission of the authors.
Satchwell, C.J. (1986) Marine Aerofoil Motion Damping and Related Propulsive Benefits, University of Southampton, Southampton. UK
Salvesen, N. (1978) Added Resistance of Ships in Waves. *J. of Hydronautics*, 12 (1), pp24-34.
Schenzle, P. (1985) Estimation of Wind Assistance Potential. *J. of Wind Engineering and Industrial Aerodynamics*, 20 (1-3), pp97-109.
Schneekluth, H. and Bertram, V. (1987) *Ship Design for Efficiency and Economy.* Butterworth-Heinemann, Oxford.
SkySails (2010) SkySails: Turn Wind into Profit. *http://www.skysails.info/.*
Walker, J.G. (1985) A High Performance Automatic Wingsail Auxiliary Propulsion System For Commercial Ships. *J. of Wind Engineering and Industrial Aerodynamics*, 20 (1-3), pp83-96.
Wärtsilä Ship Power R&D (2009) Boosting Energy Efficiency. *Presentation.*
Wärtsilä Ship Power Technology (2009) Wärtsilä 50DF Main Data. *Leaflet.*
Watson, D.G.M. and Gilfillan, A.W. (1977) Some Ship Design Methods. *Trans. RINA*, 119 p.45.
Watson, D.G.M. (1998) *Practical Ship Design.* Elsevier, Oxford.

NOMENCLATURE

Symbols:

B	Beam
C_B	Block coefficient
D	Depth
g	Acceleration due to gravity
L_{OA}	Length overall
L_{WL}	Waterline length
P_B	Brake power
R_{AW}, σ_{AW}	Added resistance, and associated coefficient
T	Draught
Δ	Displacement mass
ζ	Wave height
λ	Wavelength
ρ	Water density

Acronyms:

CRP	Contra-rotating pod
EEDI	IMO Energy Efficiency Design Index
FE	Finite element
FSAF	Fast sail assisted feeder
IMO	International Maritime Organisation
LNG	Liquefied natural gas
nm	Nautical mile
MCA	Maritime and Coastguard Agency
MCR	Maximum continuous rating
MDO	Marine diesel oil
PM	Particulate matter
PPP	Performance Prediction Program
QPC	Quasi-propulsive coefficient
SDA	Structural design procedures
S.E.	South East
SFC	Specific fuel consumption
TEI	Transport Efficiency Index
TEU	Twenty-foot equivalent unit

APPENDIX – GENERAL ARRANGEMENT DRAWING (PROFILE VIEW)